K. NOWICKA-BAUER[1], A. LEPCZYNSKI[2], M. OZGO[2], M. KAMIENICZNA[1], M. FRACZEK[1],
L. STANSKI[2], M. OLSZEWSKA[1], A. MALCHER[1], W. SKRZYPCZAK[2], M.K. KURPISZ[1]

SPERM MITOCHONDRIAL DYSFUNCTION AND OXIDATIVE STRESS AS POSSIBLE REASONS FOR ISOLATED ASTHENOZOOSPERMIA

[1]Institute of Human Genetics, Polish Academy of Sciences, Poznan, Poland; [2]Department of Physiology, Cytobiology and Proteomics, West Pomeranian University of Technology, Szczecin, Poland

Reduced sperm motility, defined as asthenozoospermia, is a frequent cause of male infertility, and is mainly connected with the dysfunction of sperm mitochondria. The aim of this study was to identify the proteins, and thereby the metabolic pathways, responsible for asthenozoospermia, using 2-DE and MALDI-TOF MS, and correlate the results obtained with those of two mitochondrial tests: JC-1 and MitoSox Red. The JC-1 test was performed to test sperm mitochondrial activity, and the MitoSox Red test was performed to check whether the observed sperm poor motility is associated with mitochondrial reactive oxygen species (ROS) production. To identify proteins strictly connected with reduced sperm motility, men with isolated asthenozoospermia (n = 4 versus 10 normozoospermic controls) alone were included in the study. The proteomic analyses resulted in the identification of 25 sperm proteins that are differentially expressed in asthenozoospermic individuals. Most of the identified proteins were downregulated and were involved in energy production; however, we have also identified structural sperm proteins and proteins secreted by the epididymis. The latter, together with the results from MitoSox Red assay, may provide insights into the pathophysiological basis of asthenozoospermia.

K e y w o r d s : *asthenozoospermia, sperm motility, sperm physiology, sperm mitochondria, normozoospermia, reactive oxygen species, proteomics*

INTRODUCTION

Infertility is a global problem that is both social and medical, affecting approximately 15% of couples (1). It is calculated that the 'male factor' accounts for up to 50% of all infertile couples (2) and is mainly associated with disorders in sperm concentration, morphology, and motility. Among them, low sperm motility is one of the most frequent types of male infertility, and affects approximately 40% of all cases (3).

Asthenozoospermia (AZS) can be a consequence of many factors. It can result from abnormal semen liquefaction, bacterial infections, or genetic defects, or be a consequence of yet unrecognized alterations at the molecular level, including proteomic changes (4-6). Possible modifications of this condition (7-9) suggest that some of these alterations can be evoked by the presence of high levels of reactive oxygen species (ROS) in the male reproductive tract (10). Increased ROS levels have been documented to be associated with distinct pathologies like varicocele, cryptorchidism, urogenital tract infection, the presence of bacteria and/or leukocytes in the semen, and others (11). It can also result from inflammation in the testes or epididymis without infiltration of leukocytes to the semen (7, 12, 13). ROS can disrupt sperm movement by peroxidation of lipids in sperm membranes, changing membrane integrity and protein composition (13) and the ROS-induced alterations have been documented visually with more elaborated methods by the other

authors (8). Moreover, the more lipid peroxidation the more of aldehydes which are secondary products of this process. Aldehydes can easily diffuse across plasma membrane and then modify any cytoplasmic or nuclear protein (14). They are also highly mutagenic species affecting mitochondrial DNA which, in turn, triggers further ROS production in these structures and more harmful aldehydes (15). The accumulation of changes in mitochondrial DNA leads to the insufficient transcription and/ or inactivation of its genes which encode several proteins from the electron transport chain. This protein alterations, together with other proteins modified by accumulating aldehydes may result in dysfunction of mitochondria and ineffective energy production.

It has also been shown that lipid sperm membrane peroxidation leads to a decrease in mitochondrial membrane potential ($\Delta\Psi$m) (16), and a relationship between the low $\Delta\Psi$m and reduced sperm motility has been well documented in the literature (17, 18). Changes in mitochondrial sperm membrane composition can affect the activity of the respiratory chain and oxidative phosphorylation (OXPHOS) pathways, leading to loss of energy production and thereby lowering sperm motility (17, 19, 20). In a proteomic study by Amaral *et al*. (20) proteins identified to be differentially expressed in low motility spermatozoa were mainly of mitochondrial and cytoplasmic origin and a great proportion of them were responsible for metabolism and energy production being involved in glycosylation, pyruvate metabolism and tricarboxylic acid cycle

(TCA), electron transfer chain or beta-oxidation. Furthermore, different tektins, heat shock proteins, proteasomal proteins and proteins of intracellular trafficking were also identified.

In the present study, we applied proteomic tools to compare sperm proteome profiles between normozoospermic (NZS) males and patients with isolated cases of AZS. To investigate a possible direct connection between the identified proteins and functional status of mitochondria, the ΔΨm was evaluated. In order to check whether possible protein alterations are connected with ROS activity, the level of mitochondrial superoxide anion secretion was investigated in both subgroups.

MATERIAL AND METHODS

Chemicals

All reagents were obtained from Sigma-Aldrich Chemie Gmbh (Munich, Germany) unless otherwise stated.

Sample collection and seminological analysis

Human semen samples were obtained from individuals volunteering to participate in our research. All experimental protocols were approved by the Local Bioethical Committee, Medical University of Poznan, Poland, and informed consent was obtained from all subjects. Semen was collected by masturbation into sterile disposable containers after 3 – 5 days of sexual abstinence, and allowed to liquefy for 30 – 60 minutes. Then, routine seminal analyses were performed according to World Health Organization (WHO) guidelines (21).

Altogether, the study included 4 sperm samples from men with diagnose of isolated AZS and 10 sperm samples from normozoospermic individuals. Men with other semen pathologies such as oligozoospermia, teratozoospermia or leukocytospermia were excluded from the study.

To avoid 'false' AZS samples, extended microbiological screening with respect to aerobic, anaerobic, and atypical bacteria was performed, as well as antisperm antibody screening.

JC-1 assay for determination of mitochondrial potential

The sperm values of mitochondrial activity (ΔΨm) in NZS and AZS individuals were determined using the cationic lipophilic dye JC-1 (5,5',6,6'-tetrachloro-1,1',3,3'-tetraethylbezimidazol-carbocyanine iodide; Molecular Probes, Inc., Eugene, OR, USA) as previously described (22). Briefly, sperm suspensions (2×10^6/ml) were incubated with 10 μg/ml JC-1 dye (20 min, 37°C, in the dark). Fluorescence was evaluated at $400 \times$ magnification under a fluorescent microscope (Olympus BX41, Tokyo, Japan) with a triple emission filter (DAPI/FITC/TexasRed), enabling the simultaneous viewing of the green JC-1 monomers (Ex/Em 490/529, indicative of loss of ΔΨm) and orange JC-1 aggregates (Ex/Em 514/590, indicative of normal ΔΨm). The mitochondrial uncoupler carbonyl cyanine p-(trifluoromethoxy)phenylhydrazone (FCCP) served as the negative control. For each individual 200 sperm cells were counted.

Detection of mitochondrial superoxide anion

In order to estimate the amount of superoxide anion produced in spermatozoal mitochondria, we used MitoSOX Red fluorochrome (Molecular Probes Inc., Eugene, OR, USA). Five NZS and four AZS sperm samples were included in this analysis. MitoSOX Red stock solution was added to the cell suspension (20 $\times 10^6$ cells per mL) to yield a final concentration of 2.5 μM. Fluorescence was measured using a Beckman Coulter flow cytometer (Cell LabQuanta™SC; Fullerton, CA, USA), and the results were expressed as the percentage of MitoSOX Red-positive cells and as the mean fluorescence intensity of MitoSOX-positive cells. 10 000 cells were examined for each experiment.

Sample preparation and protein extraction

Sperm cells were isolated from semen samples using a single layer of 50% Percoll, ($350 \times g$, 30 min) (23). Whole cell pellets were examined for the presence of other cells under a light microscope showing no contaminating leukocytes. Then, the cell pellet was resuspended and incubated for 1 hour at RT with lysis buffer (urea, thiourea, 3-[(3-cholamidopropyl) dimethylammonio]-1-propanesulfonate (CHAPS), octyl β-D-glucipyranoside, phenylmethylsulfonyl fluoride (PMSF)) (24), with the addition of 4% protease inhibitors (O'complete Protease Inhibitors Cocktail, Hoffmann-La Roche, Basel, Switzerland).

The total sperm protein concentration was measured using the RC-DC Protein Assay (Bio-Rad Laboratories, Hercules, CA, USA), with bovine serum albumin as the standard.

Two-dimensional gel electrophoresis (2-DE)

The NZS sperm protein samples, due to the relatively high number of cases, were processed in 10 biological replicates. In case of the less numerous AZS group, the samples were processed in four biological and two technical replicates. 2-DE was carried out as previously described (25). Briefly, protein samples (400 μg) were applied to pH 5 – 8, 11-cm (nonlinear) ReadyStrip™ IPG Strips (Bio-Rad Laboratories, Hercules, CA, USA). Isoelectrofocusing was performed in a total of 35,000 Vh using a Protean® i12™ IEF Cell (Bio-Rad Laboratories Hercules, CA, USA). After IEF, the IPG strips were reduced with dithiothreitol (DTT) for 15 minutes and then alkylated with iodoacetamide for 20 minutes. The second dimension was performed in 12% SDS polyacrylamide gels in total of 920 Vh at 10°C in a Protean Plus™ Dodeca Cell™ electrophoretic chamber (Bio-Rad Laboratories, Hercules, CA, USA). After 2-DE separation, the gels were stained with colloidal Coomassie Brilliant Blue G-250 according to the method of Pink *et al*. (26).

Image analysis

Image acquisition was performed using a GS-800™ Calibrated Densitometer (Bio-Rad Laboratories, Hercules, CA, USA). Analysis of the 2-D images was performed using PDQuest 8.0.1 Advanced (Bio-Rad Laboratories Hercules, CA, USA) software. To measure the variability within the group, the coefficient of variation was calculated for each replicate group. Qualitative and quantitative comparisons between the groups were performed to identify differences in protein expression pattern. Normalization was performed using a local regression model (LOESS). Experimental isoelectric point (pI) and molecular weight (Mw) were computed for each identified protein spot. Computed and theoretical values of pI and Mw were compared. Linear regression was calculated for pI, and power regression was calculated for protein Mw. Calibration for both was achieved using protein coordinates that showed minimal deviation between their theoretical and experimental pI (0.2 pH) and Mw (5 kDa) values, as described by Rogowska-Wrzesinska *et al*. (27).

Mass spectrometry

Protein spots were manually excised, and identified using a Microflex™ matrix-assisted laser desorption/ionisation-time of flight (MALDI-TOF) mass spectrometer (Bruker Daltonics, Bremen, Germany) as previously described by Ozgo *et al*. (28).

Briefly, proteins present in destained and dried spots were digested with trypsin (Promega, Madison, USA) and then extracted with 100% acetonitrile (ACN). Subsequently, Dried-Droplet crystallization was performed. The peptide mixture was loaded onto a MALDI-MSP AnchorChip™ 600/96 plate (Bruker Daltonics, Bremen Germany), mixed with the matrix solution (5 mg/ml α-cyano-4-hydroxy-cinnamic acid (HCCA), 0.1% v/v TFA, 50% v/v ACN) to yield 1 μl of suspension, and left to complete liquid evaporation. A mass spectrometer operated in a positive ion reflector mode. Mass spectra were acquired using flexControl (Bruker Daltonics, Bremen, Germany) software. Internal calibration was performed according to trypsin autolytic products (842.51 and 2211.10 *m/z*). External calibration was achieved using Peptide Calibration Standard II (Bruker Daltonics, Bremen, Germany). The obtained spectra were then processed using the flexAnalysis (Bruker Daltonics, Bremen Germany) analysis software. Peptide mass fingerprinting data were compared to mammalian databases (UniProt and NCBI) using the MASCOT search engine (http://www.matrixscience.com/). Search criteria included: trypsin, carbamidomethylation of cysteine as a fixed modification, methionine oxidation as a variable modification, mass tolerance to 150 ppm, and a maximum of one missed cleavage site.

Bioinformatic analyses of the identified proteins

Proteins identified as having altered expression in asthenozoospermic samples were categorized according to their subcellular localisations and biological functions on the basis of the UniProt Knowledgebase (UniProtKB; http://www.uniprot.org). Proteins were also classified according to their biological pathways/terms using tools of the Reactome Pathway Database (http://reactome.org) and KEGG Pathway Database (http://www.genome.jp/kegg/pathway.html). Gene ontology (GO) analysis was performed using DAVID bioinformatics software (http://david.aabcc.ncifcrf.gov/) (29).

Clustering analysis

PermutMatrix software v.1.9.3 (http://www.atgc-montpellier.fr/permutmatrix) was used to create a heat map based on the data of the expression of the sperm proteins in the healthy individuals and the asthenozoospermic patients. The data presentation for MermutMatrix analysis was performed as previously described by Lemanska-Perek *et al*. (30).

Validation study using Western blot analysis

Three proteins were selected for Western blot validation: lactotransferrin (LTF), ATP-synthase beta subunit (ATP5B), and protein deglycase (DJ-1). LTF was selected as an example of an overexpressed protein, ATP5B as an example of a downregulated mitochondrial protein, and DJ-1 as an internal control, as its decreased expression in AZS has already been documented (31). Before labelling, sperm protein samples were separated by sodium dodecyl sulphate polyacrylamide gel electrophoresis (SDS-PAGE), transferred to polyvinylidene difluoride (PVDF) membranes (Merck Millipore, Billerica, MA, USA), blocked with 5% (w/v) skimmed milk (1 hour), and incubated (4°C, overnight) with primary antibodies: LTF (#07-685, Merck Millipore, Billerica, MA, USA), ATP5B (ab14730, Abcam Cambridge, UK) and DJ-1 (ab18257, Abcam). Then, incubation (1 h, RT) with horseradish peroxidase-conjugated secondary antibodies was performed. Goat anti-rabbit IgG H&L (ab97051, Abcam) was used for LTF, DJ-1, and glyceraldehyde-3-phosphate dehydrogenase (GAPDH) proteins, and goat anti-mouse IgG (Fab specific) (A9917) for the ATP5B protein. Immune-reactive

complexes were visualised with an Amersham ECL kit (GE Healthcare Life Sciences, Little Chalfont, UK). Anti-GAPDH antibody (ab9485, Abcam) was used as a control for sample loading (32). The images were visualised in a ChemiDoc™ MP System (Bio-Rad Laboratories, Hercules, CA, USA).

The expression of LTF in seminal plasma samples from both groups under study was also compared. For that purpose, seminal plasma proteins were separated in Mini-PROTEAN® TGX Stain-Free™ gels and transferred into Trans-Blot® Turbo™ Mini PVDF membranes using the Trans-Blot Turbo apparatus (Bio-Rad Laboratories Hercules, CA, USA). The relative quantity of LTF was normalized against the total protein value for each sample using the ChemiDoc XRS + system (Bio-Rad Laboratories, Hercules, CA, USA) which allowed for accurate analysis.

Immunofluorescent quantitative assessment of protein expression in spermatozoa: validation study

After semen liquefaction, a portion of semen was spread onto glass slides. The sperm samples were fixed in a solution of either: methanol or 4% paraformaldehyde (PFA), and left until use.

Fixed spermatozoa were incubated with 0.5% Triton X-100 and blocked in 2% (w/v) skimmed milk Then, the sperm samples were incubated (4°C, overnight) with the following antibodies: anti-LTF (1:200, #07-685, Merck Millipore, Billerica, MA, USA), anti-ATP5B (1:50, ab14730, Abcam), and anti- DJ-1 (1:100, ab18257, Abcam). Subsequently, samples were incubated (30 min, RT) with secondary antibodies conjugated with Alexa Fluor® 488 dye (for LTF and DJ-1, Goat Anti-Rabbit IgG H&L (ab150077, Abcam) and for ATP5B, Goat Anti-Mouse IgG H&L (ab150113, Abcam)). The control samples were prepared in the same way but without the addition of primary antibody. The sample complexes were stained with DAPI, and immunofluorescence was observed at 1000 × or 1500 × magnification under a fluorescence microscope (Zeiss Axio Observer Z1or Olympus BX41).

Statistical analysis

Statistical analysis was carried out using STATISTICA 10 or GraphPad Prism 7 software. Comparison between the NZS and AZS groups was performed using Student's t test, the Mann-Whitney U test or the two-way ANOVA test. P-values < 0.05 were considered to be significant.

RESULTS

Semen parameters and screening tests

The results of seminological analyses are presented in *Table 1*. In the AZS group, only the parameters of sperm progressive motility and total motility were below WHO criteria (21). Statistical analysis showed that these parameters, together with sperm vitality, were significantly lower in the group of infertile AZS males. Microbiological screening did not reveal any bacteriospermia in samples selected from AZS individuals, confirming that the low sperm motility was not due to a microbiological infection. The mean percentages (%) of sperm with active ΔΨm (orange fluorescence) were 71.03 ± 11.28 and 35.58 ± 8.42 in the NZS versus AZS groups, respectively, and were statistically significant different (P < 0.05, *Table 1*).

The mean percentages of MitoSOX-positive cells in the NZS and AZS groups were 9.2% (± 2.37) and 22.005% (± 6.44), respectively, and the values obtained also showed statistically significant differences (P < 0.005, *Table 1*).

*Table 1*. Results of semen human parameter analysis including mitochondrial function.

Parameters studied	Normozoospermia	Asthenozoospermia
Age of patients	31.4 ± 7.18	31.25 ± 7.5
Ejaculate volume (ml)	3.1 ± 0.68	2.49 ± 0.64
Sperm concentration (× 10^6/ml)	124.03 ± 79.1	65.34 ± 20.65
Progresive motility (A+B) (%)*	59.87 ± 11.27	25.11 ± 8.81
Total motility*	72.2 ± 10.86	37.98 ± 9.87
Sperm vitality (%)*	84.9 ± 7.38	68.87 ±10.12
Good sperm morphology (%)	8.5 ± 4.3	6.5 ± 1.73
JC-1 test (%)*	71.03 ± 11.28	35.58 ± 8.42
MitoSox Red test (%)**	9.2 ± 2.37	22.005 ± 6.44

Data are presented as mean ± S.D. *indicates parameters with $P < 0.05$ and ** with $P < 0.005$ of statistical significance in t-Student or Mann-Whitney U tests; SD, standard deviation.

Table 2. Protein characteristics in spermatozoa of asthenozoospermic males.

Spot no.	Accesion number UniProt/NCBI	Protein name	Gene name	Ratio astheno/ normo	Sequence coverage/M ASCOT score	Peptides matched	SL	BP	Theo. pI/Mw	Exp. pI/Mw
Down-regulated proteins										
41	Q96BH3	Epididymal sperm-binding protein 1	ELSPBP1	0.209	47/63	5	S	SM	6.20/27.00	6.6/30.2
44	Q13011	Delta(3,5)-Delta(2,4)-dienoyl-CoA isomerase, mitochondrial	ECH1	0.352	41/84	8	MT	ME	8.16/36.14	7.0/31.7
7	NP_001229283	Outer dense fiber protein 2 isoform 8	ODF2	0.425	41/196	30	FL	STS	7.27/67.32	6.0/84.4
26	P78371	T-complex protein 1 subunit beta	CCT2	0.425	54/189	21	CT	PM	6.01/57.80	6.7/54.5
5	Q5BJF6	Outer dense fiber protein 2	ODF2	0.463	23/104	18	FL	STS	7.53/96.14	5.8/90.7
46	Q99497	Protein deglycase DJ-1	PARK7	0.521	37/77	5	CM	MM	6.33/20.05	6.6/24.4
31	P16219	Short-chain specific acyl-CoA dehydrogenase, mitochondrial	ACADS	0.540	55/156	14	MT	ME	8.13/44.61	6.9/39.5
14	P06576	ATP synthase subunit beta, mitochondrial	ATP5B	0.566	70/334	30	MT	ME	5.26/56.52	5.3/53.9
15	P06576	ATP synthase subunit beta, mitochondrial	ATP5B	0.589	63/201	20	MT	ME	5.26/56.52	5.4/55.1
16	Q9UIF3	Tektin-2	TEKT2	0.648	47/130	13	FL	STS	5.39/50.15	5.8/52.1
20	P49189	4-trimethylaminobutyraldehyde dehydrogenase	ALDH9A1	0.661	43/173	18	CT	ME	5.69/54.68	6.0/49.6
18	Q14410	Glycerol kinase 2	GK2	0.663	44/185	18	MT	ME	5.57/61.41	5.9/52.0
35	P50213	Isocitrate dehydrogenase [NAD] subunit alpha, mitochondrial isoform X2	IDH3A	0.677	39/119	15	MT	ME	6.02/34.94	6.0/41.3
24	P55809	Succinyl-CoA:3-ketoacid coenzyme A transferase 1, mitochondrial	OXCT1	0.705	29/70	8	MT	ME	7.14/56.58	6.7/57.3
23	Q9P2R7	Succinyl-CoA ligase [ADP-forming] subunit beta, mitochondrial	SUCLA2	0.706	41/161	20	MT	ME	5.84/46.73	6.2/45.4
21	XP_005252087	Outer dense fiber protein 2 isoform X21	ODF2	0.724	30/104	23	FL	STS	5.61/74.69	6.2/55.2
32	P16219	Short-chain specific acyl-CoA dehydrogenase, mitochondrial	ACADS	0.735	47/92	12	MT	ME	8.13/44.61	6.7/40.6
27	P68371	Tubulin beta-4B chain	TUBB4B	0.738	40/90	12	CS	IT	4.79/50.25	6.7/45.1
12	P34931	Heat shock 70 kDa protein 1-like	HSPA1L	0.749	34/99	18	CT	PM	5.76/70.73	6.1/74.3
17	Q969V4	Tektin-1	TEKT1	0.790	49/199	12	FL	STS	5.98/48.28	5.8/52.1
Up-regulated proteins										
29	P15104	Glutamine synthetase	GLUL	1.270	33/161	13	CT	PM	6.43/42.66	7.0/43.9
50	P25787	Proteasome subunit alpha type-2	PSMA2	1.841	44/103	7	CT	PM	7.08/24.97	7.2/22.7
10	P31040	Succinate dehydrogenase [ubiquinone] flavoprotein subunit, mitochondrial	SDHA	1.874	42/171	23	MT	ME	7.06/73.67	6.6/72.0
39	P11177	Pyruvate dehydrogenase E1 component subunit beta, mitochondrial	PDHB	2.409	39/62	8	MT	ME	6.20/39.55	6.1/29.0
4	P28331	NADH-ubiquinone oxidoreductase 75 kDa subunit, mitochondrial	NDUS1	2.907	45/282	28	MT	ME	5.89/80.44	5.7/88.4
6	P02788	Lactotransferrin	LTF	3.472	36/144	23	S	IM	8.50/80.01	6.0/89.3
8	Q5JQC9	A-kinase anchor protein 4	AKAP4	3.522	28/95	21	FL	STS	6.56/95.84	7.2/80.7

Theo, theoretical; Exp, experimental; SL, subcellular localisation; MT, mitochondrion; CT, cytoplasm; CM, cell metabolism; FL, flagellum; S, secreted; CS, cytoskeleton; BP, biological process; ME, metabolism and energy production; PM, protein metabolism; STS, sperm tail structure and motility; SM, spermatogenesis and sperm maturation; MM, mitochondrial maintenance; IT, intracellular trafficking; IM, immunity.
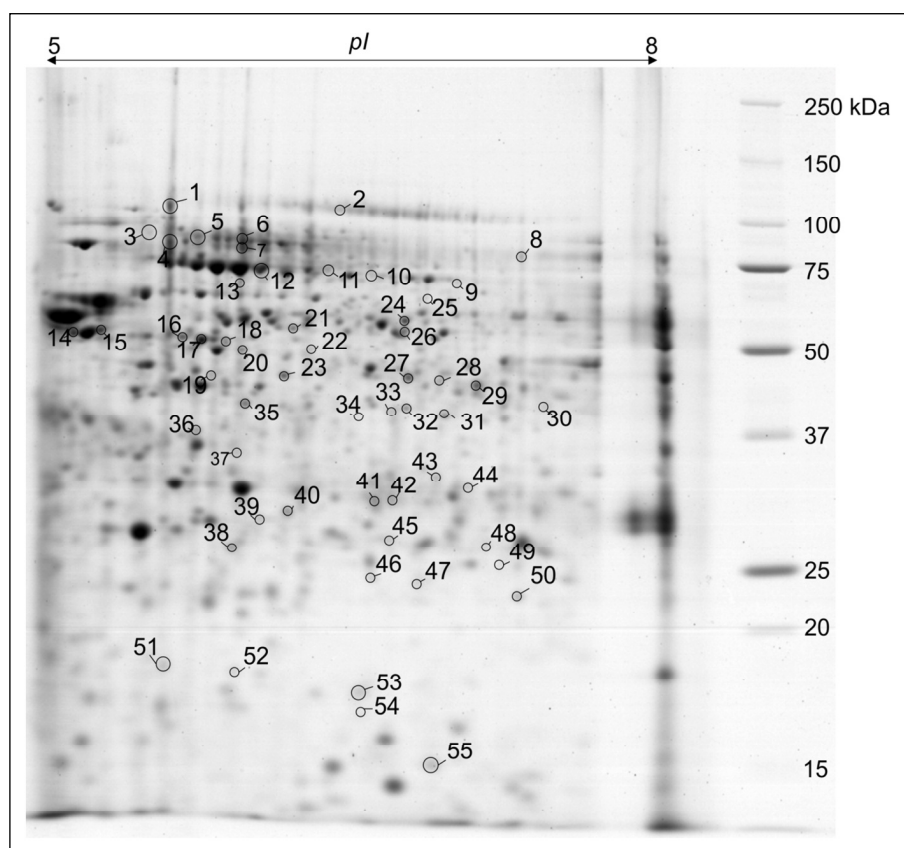
Fig. 1. Master 2-D gel with separated human sperm proteins stained with colloidal Coomassie Brilliant Blue G-250. Enircled are protein spots that were differentially expressed in the asthenozoospermic group and were subjected to MALDI-TOF MS identification.

Gel imaging and spot distribution

Comparative analysis of sperm proteins from NZS and AZS samples by means of 2-DE resulted in the identification of 55 differentially expressed protein spots. Because of the analysis of pI and Mw each of the identified differentially expressed protein spots were experimentally computed and compared to the theoretical values available in databases such as ExPASy and NCBI (*Table 2*). All of the spots analysed were characterized by pI values ranging between 5 and 8, and Mw values between 22.3 and 85.0 kDa (*Fig. 1*). A variation coefficient was estimated for both groups and reached 62.75% in NZS and 61.32% in AZS samples.

For setting the spot distribution, all coordinates were plotted after calibration of the Mw and pI scales using protein spots that showed minimal deviation between their theoretical and experimental pI and Mw values. Analysis has shown that the discrepancies between theoretical and experimental values are more frequent and higher for pI than for Mw values. Among the 27 identified protein spots, seven were classified as pI outliers (*Fig. 2*), these were LTF (spot 6), outer dense fibre protein 2 (ODF2, spots 5 and 7), mitochondrial short-chain specific acyl-CoA dehydrogenase (SCAD, spots 31 and 32), mitochondrial (3,5)-delta(2,4)-dienoyl-CoA isomerase (ECH1, spot 44), and tubulin beta-4B chain (TUBB4B, spot 27).

Protein identification and quantification

Fifty-five protein spots with altered expression were excised from the gels and analysed by MALDI-TOF MS. As a result, 25 unique sperm proteins represented in 27 spots were identified. Among them, 18 proteins were downregulated and 7 were upregulated, compared to NZS (*Table 2*). The ratios of protein levels in AZS to those in NZS samples ranged from 0.209 to 3.522.

According to information available at UniProtKB, most of the identified proteins are of mitochondrial origin, while the other proteins are localised in the cytoplasm, cytoskeleton, or cell membranes, or are connected with cell secretions (*Fig. 3A*). Analysis of the identified proteins with reference to their biological function showed that the vast majority of the identified proteins were engaged in cell metabolism and energy production. Other identified proteins were found to be involved in sperm tail structure/motility, protein metabolism, mitochondrial maintenance, spermatogenesis, sperm maturation, intracellular trafficking, and immunity (*Fig. 3B*).

Bioinformatics analysis by Reactome, KEGG and GO revealed that proteins identified in our study were mainly connected with energy metabolism and structure (*Table 3*). Proteins with altered expression were mainly involved in the tricarboxylic acid (TCA) cycle; OXPHOS; pyruvate, butanoate, and propanoate metabolism, and in structures connected with sperm motility.

Comparative visualisation of the levels of differentially expressed proteins in the two analysed groups of males is presented as a heat map (*Fig. 4*). Two differentially expressed groups of proteins (up- and downregulated in AZS) can be clearly distinguished with the prevalence of downregulated proteins (in AZS samples).

Western blot analysis

Western blotting analysis validated the previous results and showed the same trends as seen in the comparative analysis of the 2-DE maps: significant upregulation of LTF and downregulation of ATP5B and DJ-1 (*Figs. 5A* and *5B*) in AZS individuals. Comparison of seminal plasma LTF levels from both studied subgroups did not reveal any significant differences (*Fig. 6*).
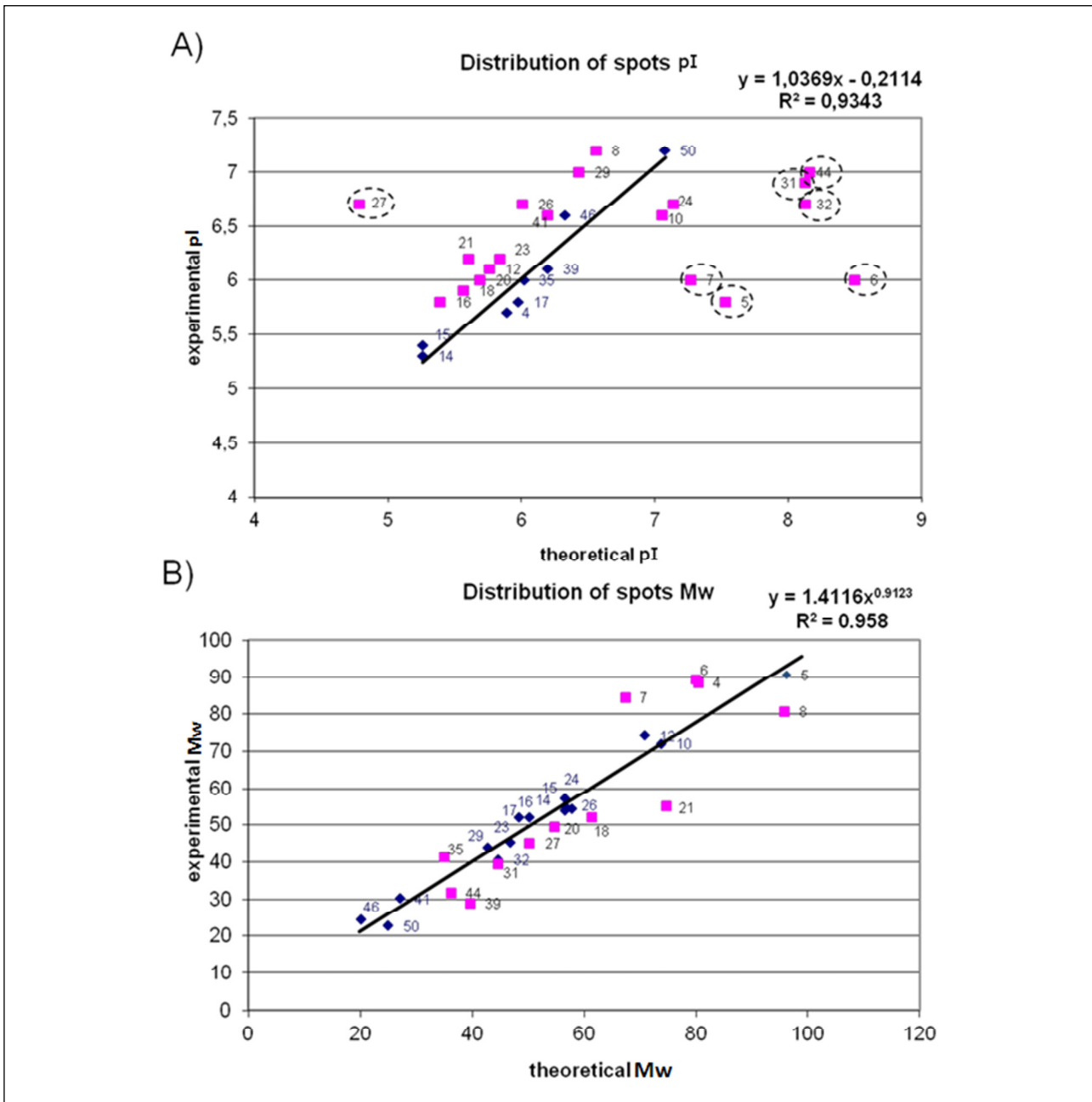
Fig. 2. Graphs representing the distribution of protein spots according to their pIs and Mws. Analysis of theoretical and experimental pI and Mw values revealed seven protein spots classified as pI outliers. These outlier spots were represented by the following five distinct proteins: LTF, ODF2, SCAD, ECH1, and TUBB4B. Human LTF is a basic sperm protein with a pI of 8.5 and Mw of 80 kDa. In the present study, the pI of the spot representing this protein was computed to be 6.0. According to the conclusions of Majka *et al*. (33), the observed pI of the LTF similar to transferrin can be noticeably decreased both as a consequence of increasing in the number of glycosylated arginine residues and upon its saturation with iron. Saturation of this protein with iron is the most probable reason for the observed decreased pI. It should be emphasized that in semen, iron serves as a catalyst in the production of reactive oxygen species (34). Additionally, in 2-D gels of elephant seminal plasma, Kiso *et al*. (35) have observed the LTF as a train of spots with a range of pH values from approximately 5.0 to 10.0. In this study, two spots representing ODF2 have also been found as pI outliers. For both these spots, the experimental pIs were lower than those predicted in databases. These differences can be connected with the phosphorylation of amino acid residues, which is the most common post-translational protein modification (PTM), and it is known to decrease the pH. According to the PhosphoSite database (http://www.phosphosite.org/), phosphorylation of 12 and 16 residues decreased the ODF2 pI down to 5.99 and 5.78, respectively. SCAD is another protein referred to as a pI outlier in our study. The difference between the theoretical and experimental pI values can be due to the cleavage of peptide bonds. For SCAD proteins, their cytoplasmic precursor form (pI = 8.13) is transferred into a mitochondrion, where proteolytic cleavage of a 2.5-kDa entity rich in basic amino acids converts it into the mature form with a pI of 6.15 (36, 37), which is similar to the values observed in our study (spot 31, pI = 6.9; spot 32, pI = 6.7) as well as to proteomic profiling of human testis (7.29) and kidney (6.41) (38, 39). Another pI shift has been observed for the ECH1 protein spot. According to the ExPASy database, the predicted pI of this protein is 8.16. However, it should be noted that after the cleavage of the signalling 33-amino acid peptide, its pI decreases to 6.00. In a study by Friry-Santini *et al*. (39), the pI of the protein spot representing ECH1 (7.09) was almost the same as that observed in our study.
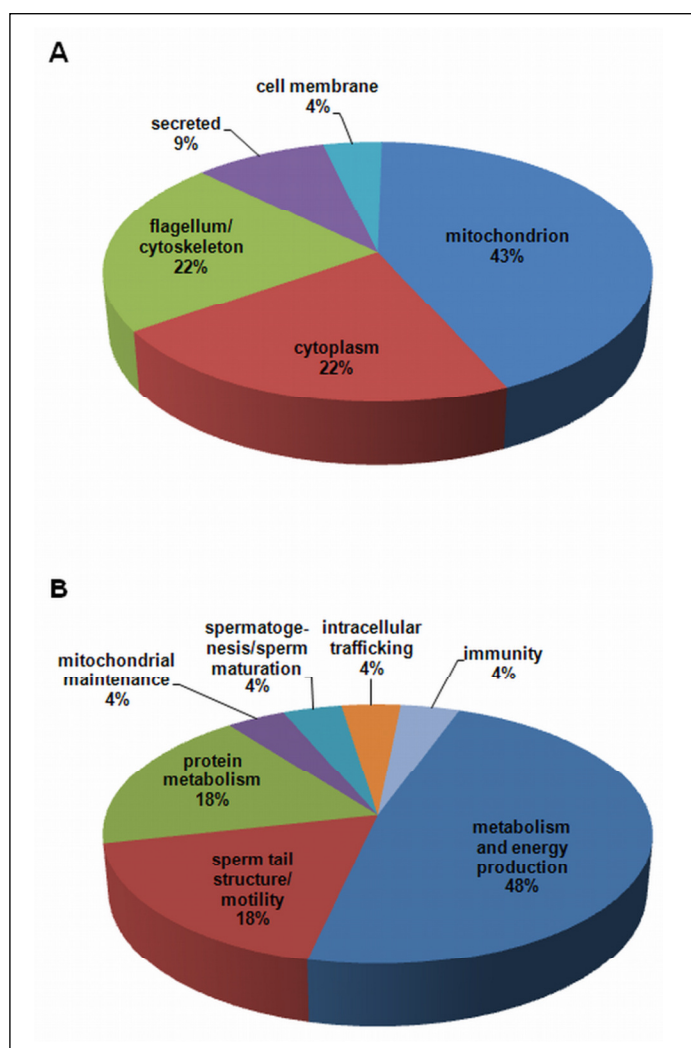
Fig. 3. Classification of differentially expressed human sperm proteins according to their subcellular localisation (A) and cellular function (B).

Immunofluorescent assessment of protein expression

Fluorescent microscopy was used to visualise the localisation of the LTF, ATP5B, and DJ-1 proteins in NZS (n = 2) and AZS (n = 2) sperm samples. The results indicated that in AZS sperm cells, the LTF signal was strongly localised in the equatorial region of the sperm head (69.4% of sperm cell population), whereas in NZS samples, the observed signal was much more discrete (80% of sperm cells) (*Fig. 7A*). Unlike in the NZS sample, staining was also localised at the base of the sperm head (13.3%), in the midpiece (24.5%), between the midpiece and the principal piece (20.4%), and at the end piece of the spermatozoa (5%). The staining of two mitochondrial proteins, DJ-1 and ATP5B, was observed in the sperm midpiece (56.3% in NZS and 50.4% in AZS for DJ-1 and 80.6% in NZS and 95.8% in AZS for ATP5B), however, the signal was significantly lower in the AZS group *(Fig. 7B* and *7C)*. Additionally, in contrast to AZS patients, DJ-1 protein expression was also visible along the whole sperm tail in NZS samples (42.8% of sperm cells).

DISCUSSION

The aim of this study was to identify human sperm proteins and biochemical pathways affected in isolated AZS by comparing proteomic profiles between NZS males and individuals with poor sperm motility. Because the main changes in AZS were documented to be associated with sperm mitochondria (14), we investigated ΔΨm and the level of mitochondrial superoxide anion secretion to identify any correlations between proteomic and sperm functional data.

The MALDI-TOF MS analysis resulted in the identification of 25 differentially expressed sperm proteins in men with isolated AZS (*Table 2*). Most of these proteins (18) were downregulated and were located in the sperm mitochondrion (43%) (*Table 2*, *Fig. 3A*). A significant proportion of the identified proteins (48%) were involved in metabolism and energy production (*Fig. 1B*). This finding, together with the mitochondrial localisation of the identified proteins, confirmed the results from the JC-1 test (*Table 1*) and is consistent with the report by Amaral *et al.* (20).

Classification of the identified proteins by the tools of the GO, Reactome, and KEGG pathways indicated that sperm mitochondrial proteins with altered expression in AZS have been responsible for the generation and integration of metabolites and energy, and they were involved in the TCA cycle, OXPHOS and the metabolism of butanoates, propanoates, and pyruvates (*Table 3*). Mitochondrial proteins found in our research as dysregulated in isolated AZS are presented in *Fig. 8*.

Pyruvates serve as substrates for TCA cycle. Before entering this cycle they are converted into acetyl-CoA in the pyruvate dehydrogenase complex (PDC). In our study, we have found beta subunit of this complex (PDHE1-B) to be upregulated in
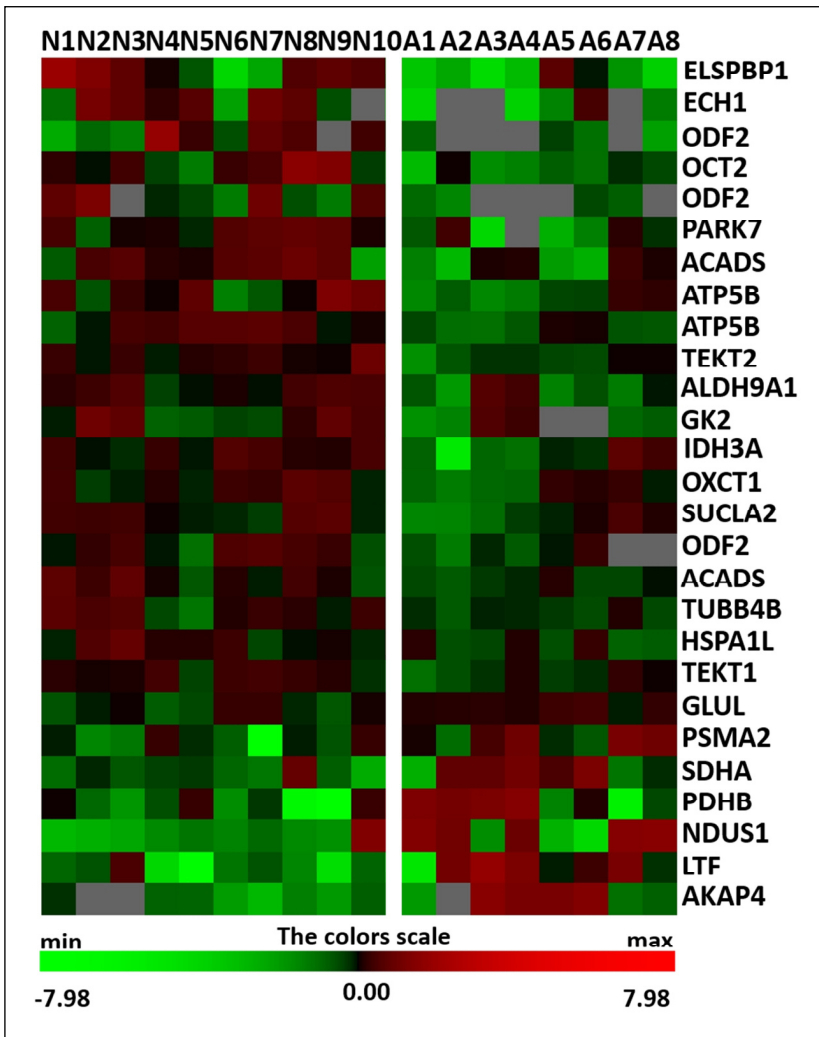
Fig. 4. In the presented heat map, normozoospermic protein samples were processed in 10 biological replicates (N1-N10), whereas asthenozoospermic samples were processed in 4 biological and 2 technical replicates (A1–A8). The differences in protein expression are clearly visible for each replicate, with a predomination of downregulated proteins in the asthenozoospermic group.

low-motility sperm in our study (*Fig. 8*) what, however, is not consistent with the results published by Amaral *et al.* (20). After conversion, acetyl-CoA enters TCA cycle. The main role of this cycle is generation of energy in a form of adenosine triphosphate (ATP). In our research we have found 2 new proteins from this cycle to be deregulated in AZS, namely: succinyl-CoA ligase (ADP-forming) beta subunit (SUCLA2, downregulated) and succinate dehydrogenase (ubiquinone) flavoprotein subunit (SDHA, upregulated) (*Table 2*, *Fig. 8*). The last protein, succinate dehydrogenase (SDH), is an enzyme that participates in both the TCA cycle and in the electron transport chain (complex II) that enables OXPHOS in mitochondria. The upregulated flavoprotein subunit (SDHA) contains flavin adenine dinucleotide and also generates chemical energy but in the form of $NADH_2$. An another upregulated protein involved in OXPHOS is the NADH-ubiquinone oxidoreductase 75 kDa subunit (NDUS1). This enzyme forms complex I of the electron transport chain. Unlike complex II, complex I also functions as a pump, transporting protons across the mitochondrial membrane using energy released during the electron transport chain and generating a proton gradient required for the maintenance of $\Delta\Psi m$. This type of energy is also used to transport protons across the inner mitochondrial membrane through the ATP-synthase enzyme (complex V), generating potential energy and electrical potential, which, due to ATP-synthase activity, is transformed into ATP necessary for sperm movement.

Nevertheless, in our work, we have also identified other mitochondrial proteins and pathways that are dysfunctional in AZS, and they all are involved in the production of energy that is required for sperm movement (*Fig. 8*).

Interestingly, bioinformatic analysis of the identified proteins by the KEGG Pathway Database indicated low expression levels of enzymes involved in butanoate and propanoate metabolism (*Table 3*), which are connected with energy generation. These results may suggest new metabolic pathways involved in sperm motility, indicating that dysfunctions in these pathways also might contribute to AZS. Further on, comparative proteomic analysis identified additional differentially expressed mitochondrial proteins that were not included in the bioinformatic analysis. Among these were proteins responsible for β-oxidation: delta(3,5)-delta(2,4)-dienoyl-CoA isomerase (ECH1) and short-chain specific acyl-CoA dehydrogenase (ACADS) (*Table 2*). The importance of this pathway for sperm motility was documented in functional, proteomic, and *in silico* studies (5, 20, 40). Finally, another mitochondrial protein is glycerol kinase 2 (GK2) (*Table 2*). This protein is anchored to the mitochondrial outer membrane and is responsible for glycerol degradation. In mice, Gk2 has been documented to play a role in sperm mitochondrial sheath formation, and Gk2-deficient mice displayed higher concentrations of ATP in their spermatozoa (41). In our work, GK2 was found to be downregulated in the sperm cells of AZS males, whereas in a work of Shen *et al.* (42) this protein was
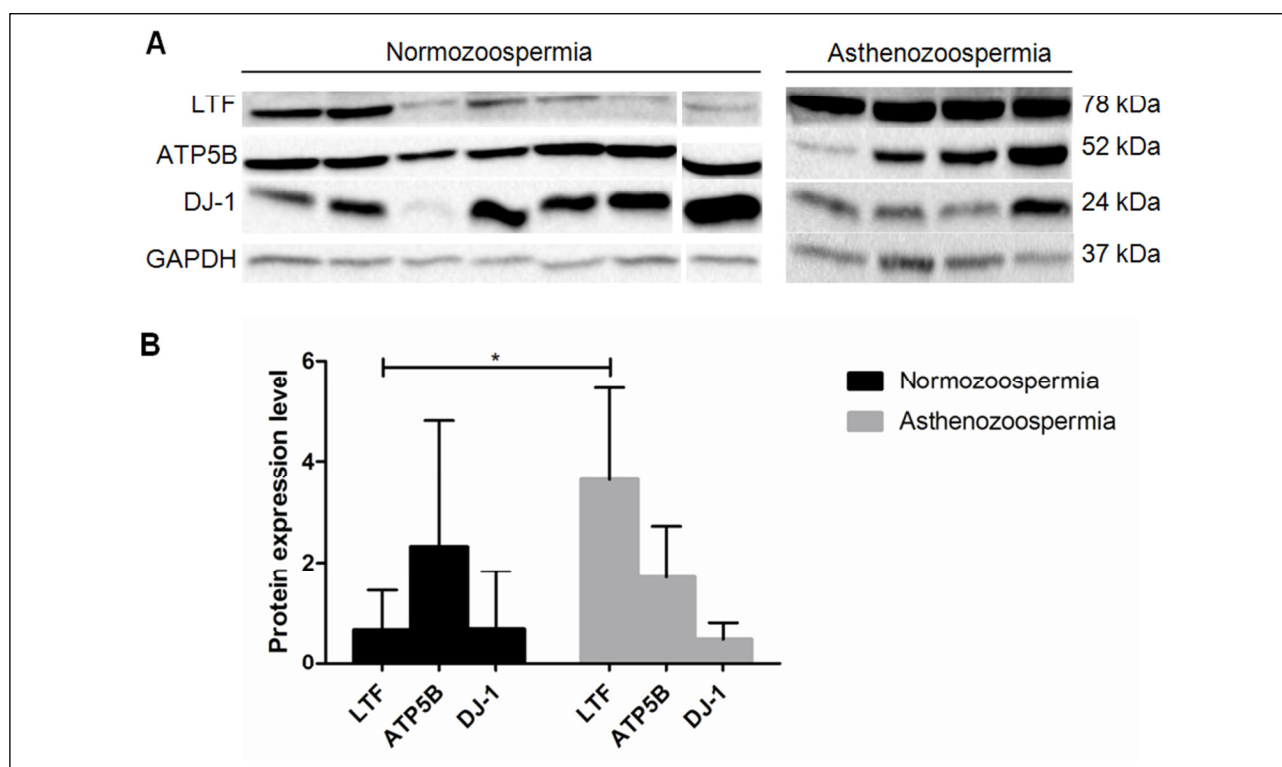
Fig. 5. (A) Western blot analysis of LTF, ATP5B, and PARK7 proteins in normozoospermic (n = 7) and asthenozoospermic (n = 4) individuals. Spermatozoa from asthenozoospermic men showed lower levels of ATP5B and PARK7 proteins and significantly stronger band intensity of LTF compared to normozoospermic men. GAPDH was used for normalization. All four proteins were detected in the same membrane, to which they were transferred from the same gel (i.e. from the same protein separation), containing control and asthenozoospermic samples. (B) A bar graph presenting expression level of LTF, ATP5B and DJ-1 proteins. In Western blot analysis only the level of LTF expression was significantly different between NZS and AZS samples ($P < 0.05$).
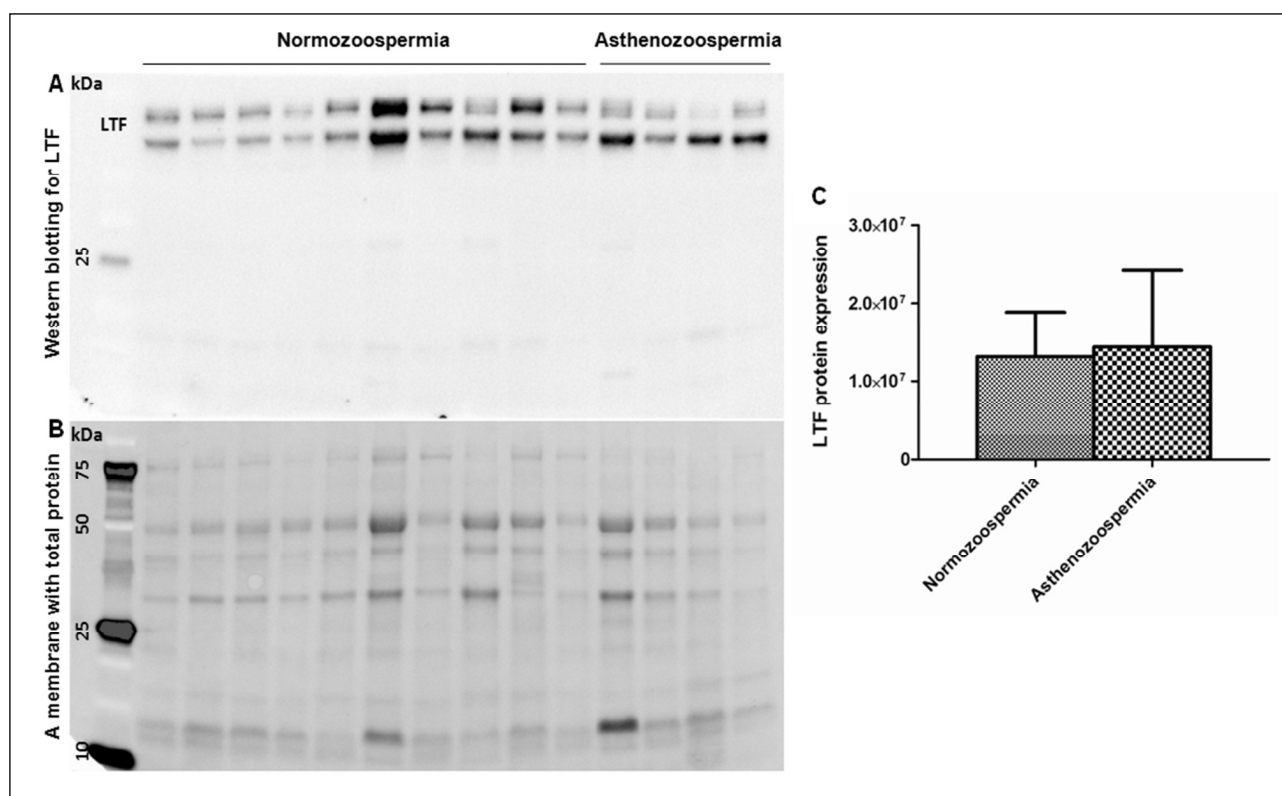
Fig. 6. Western immunoblotting for LTF in human seminal plasma. The protein was examined in the control and asthenozoospermic group (A). The level of LTF expression was normalized against the total protein value detected in the PVDF membrane (B) and is presented in the bar graph (C).
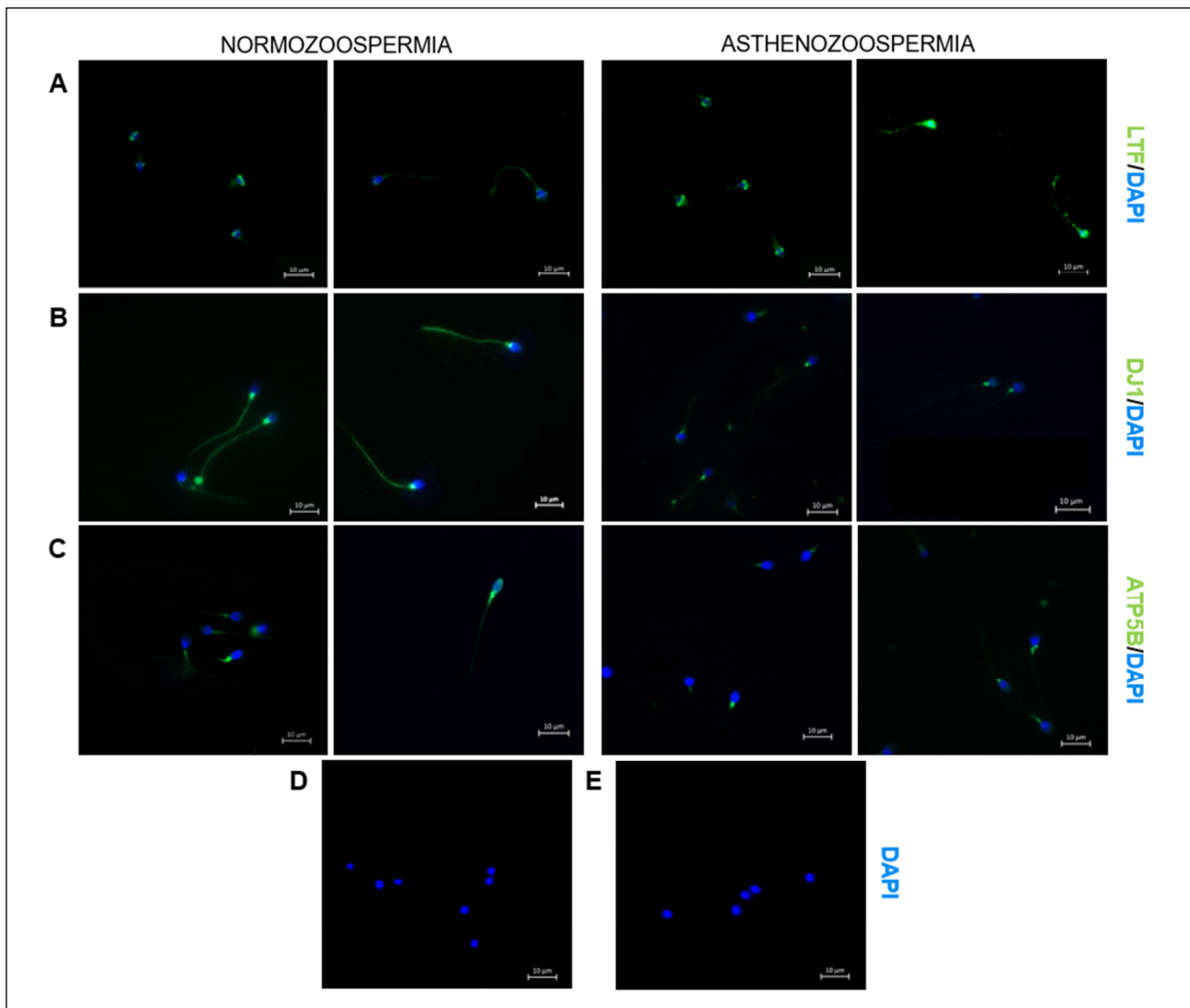
Fig. 7. Immunofluorescent localisation of LTF, DJ-1 and ATP5B proteins in human spermatozoa fixed with methanol (LTF) and 4% PFA solution (DJ-1 and ATP5B). (*A*) In normozoospermic sample, LTF was localised in the equatorial segment of the sperm head, whereas in asthenozoospermic samples, the staining localised within the equatorial segment appeared much stronger, and was also visible in the midpiece, between the midpiece and the principal piece, and at the end piece of spermatozoa. (*B*), (*C*) For the proteins DJ-1 and ATP5B, the staining was drastically weaker in the asthenozoospermic sperm and was strictly localised to the midpiece. In normozoospermia, staining for DJ-1 was visible along the sperm tail (*B*). Bar: 10 µm. (*D*), (*E*). Negative controls were incubated with secondary antibodies conjugated with Alexa Fluor® 488 dye (Goat Anti-Rabbit IgG H&L (ab150077, Abcam) and Goat Anti-Mouse IgG H&L (ab150113, Abcam)), respectively.

upregulated in AZS. However, our findings are in accordance with results of others (40, 41), suggesting that not only glycolysis, the TCA cycle, and OXPHOS are involved in energy production and therefore sperm motility. Nonetheless, our data also clearly show that not only mitochondrial proteins are deregulated in isolated AZS.

Although samples with abnormal sperm morphology were excluded from our research, we were able to identify several sperm tail proteins that demonstrated altered expression in the AZS group (*Table 2*). The identification of such a group of proteins showed that the changes brought about by their altered expression were not visible and could not be detected during a routine morphological test. These proteins included ODFs, tektins 1 (TEKT1), and 2 (TEKT2), and A-kinase anchored protein 4 (AKAP4, *Table 2*). The decreased expression of ODFs, TEKT1 and TEKT2 in asthenozoospermia has already been documented in the literature (20, 43, 44), however our results about the

upregulated expression of AKAP4 protein are in contrast to a report by Hashemitabar *et al.* (45). AKAP4 belongs to a group of proteins (A-kinase anchored proteins, AKAPs) that bind to the regulatory subunit of protein kinase A (PKA) and is a major structural component of the fibrous sheath in sperm (46, 47).

In this study, we have further identified three proteins - LTF, epididimal sperm-binding protein 1 (ELSPBP1) and DJ-1 - that are secreted in the epididymis. None of these were involved in sperm metabolism or were structural proteins; however, in our view, they together deserve some attention.

LTF is a glycoprotein that was reported to be synthesized in the epididymis in mammals (48) and has been detected in the prostate and seminal vesicles in humans (49). In the male reproductive tract, it adheres to the sperm surface *via* its receptor (LFR), which has been documented to be present in the head and midpiece of human sperm (50). Reported data correlate with our findings, which indicate that the signal from LTF was found to be

Table 3. Cellular pathways and Gene Ontology identified in asthenozoospermic samples.

Category	Pathway/term	Identifer	Gene names	Adjusted P-value (Benjamini correction)
Reactome pathway	Integration of energy metabolism	REACT_1505	*ATP5B* *NDUS1* *IDH3A* *PDHB* *SDHA* *SUCLA2*	8.0×10^{-3}
	Pyruvate metabolism and TCA cycle	REACT_1046	*IDH3A* *PDHB* *SSHA* *SUCLA2*	2.2×10^{-3}
KEGG_PATHWAY	Citrate cycle (TCA cycle)	hsa_00020	*IDH3A* *PDHB* *SDHA* *SUCLA2*	2.2×10^{-3}
	Oxidative phosphorylation	hsa_00190	*ATP5B* *NDUS1* *SDHA*	2.6×10^{-1}
	Butanoate metabolism	hsa_00650	*OXCT1* *ACADS* *ALDH9A1* *PDHB*	1.5×10^{-3}
	Propanoate metabolism	hsa_00640	*ALDH9A1* *SUCLA2*	3.2×10^{-1}
Gene Ontology Term Biological Process (GO_BP_FAT)	Generation of precursor metabolites and energy	GO:0006091	*ATP5B* *NDUS1* *ECH1* *IDH3A* *PDHB* *SDHA* *SUCLA2*	1.4×10^{-3}
	Sperm motility	GO:0030317	*AKAP4* *TEKT2*	5.8×10^{-1}

P-values < 0.05 after Benjamini correction were considered to be statistically significant.

present in the equatorial segment of the sperm head (*Fig. 7A*). LTF has the capacity to bind iron, thus confirming its antioxidant and antibacterial activities. We observed that the expression of LTF was clearly upregulated in AZS sperm samples (*Table 2*, *Figs. 5* and *7*); however, this finding completely differs from the results obtained by Shen *et al.* (42) in which there was no LTF observed in AZS sperm samples. Nevertheless, higher expression of LTF in AZS sperm samples is possible, and can be connected with its antioxidant activity. Indeed, in our study, the level of mitochondrial superoxide anion was significantly higher in AZS men than in controls (*Table 1*). However, this data can be perceived as controversial; in a study by Hamada *et al.* (51) the expression of LTF was found to be increased in spermatozoa with physiological, but not pathological ROS levels. To obtain a better understanding, we also checked the level of seminal plasma LTF in both the studied groups, and observed no statistical difference in LTF levels between seminal plasma samples from NZS and AZS individuals (*Fig. 6*). However, our findings are in partial agreement with data obtained by Sharma *et al.* (52), in which the level of LTF was uniquely expressed in seminal plasma samples with increased oxidative stress. *Prima facie*, most of these data are not coherent; however, they may in fact reflect a real dynamic situation in the epididymis and semen. It could be speculated that

the high levels of LTF tell about good condition of an organism that can actively express its gene and overcome oxidative stress. Low levels of LTF may suggest about problems with its expression and/ or transcription at the molecular level, might be connected with other accompanying disturbances in sperm, or may be caused by insufficient expression of its receptor providing self-protection. Nonetheless, all the data evidently show that LTF is involved in regulation of sperm motility *via* its antioxidant properties. It has been documented that the treatment of AZS males (evoked by the presence of leukocytes in semen as a possible source of ROS) with LTF, combined with other natural antioxidants, significantly improved the motility of sperm cells (53). Thus, it is possible that increased LTF production might be a self-protective mechanism in AZS patients. This can be in an accordance with previous findings (9) indicating the up-regulation of some seminal plasma proteins engaged in stress response in patients with idiopathic oligoasthenoteratozoospermia during elevated level of oxidative stress.

The next epididymal protein, ELSPBP1, was also downregulated in our study in sperm with low-motility (*Table 2*), similar to observations of the fraction of non-migrating spermatozoa reported by Amaral *et al.* (20). This protein is secreted by the cauda epididymis, which is a place in which

Fig. 8. The scheme presents a model of a sperm mitochondrion with marked dysfunctional metabolic pathways in asthenozoospermia. The proteins/protein subunits identified in our study as being downregulated are indicated in red, and protein subunits identified as being upregulated are indicated in green.

spermatozoa acquire their movement ability. ELSPBP1 can be bound to sperm during ejaculation and has been suggested to be involved in sperm capacitation (54).

Another protein that is downregulated in isolated AZS and is secreted in the epididymis is DJ-1. Its low level in spermatozoa with reduced motility has been well documented in the literature (31, 42, 45) and in our study, we have confirmed it by three different techniques: 2-DE, Western blotting, and immunofluorescence (*Table 2*, *Figs*. *5* and *7B*). We have also confirmed a positive correlation between DJ-1 level and ΔΨm in sperm (55). It was documented that DJ-1 has anti-oxidative properties and protects cells against hydrogen peroxide-induced cell death (56). Low amounts of this protein were also found in the seminal plasma of AZS men (50), which suggests that a decreased level of DJ-1 can be evoked by disturbances occurring in the epididymis (55).

The disrupted secretion of the epididymal proteins mentioned above might reflect a pathological condition in the epididymis connected with the presence of ROS. This situation may not only influence ROS-induced AZS but also ROS-induced oligozoospermia (low sperm concentration) which was clearly visible in seminological analyses, with a tendency to decreased sperm count in AZS samples (*Table 1*).

In this discussion we have pointed out proteins of which expression level in our work was different than in the other studies: PDHE1-B (20), AKAP4 (45), GK2 (42) and LTF (42). These different results can suggest that the reaction of an organism can vary among the subjects, at least in respect to certain proteins, and can depend on its current condition. However, the expression among replicates was rather coherent and none of them displayed an opposite pattern of expression (*Fig. 4*). From the molecular point of view, such differences can also result from posttranslational modifications which can change the quantitative protein analysis.

It is also worth of mentioning that according to the literature the mechanisms of asthenozoospermia described above are not the only ones underlying this sperm pathology. It seems that the reduced sperm motility also can be observed during seasoning (57, 58). This fluctuations can partially be correlated with changes in melatonin expression (59). Melatonin is a wide-spectrum antioxidant secreted by pineal gland and its secretion depends on daylight-fluctuations and the highest is during the dark periods. The involvement of this hormone in prooxidant-antioxidant balance can be significant and thus can affect sperm motility (60, 61). Further, the expression of melatonin can be also associated with the activation of metalloproteinases during oxidative stress

conditions (60, 62). It has been suggested that metalloproteinases together with prostate-specific antigen and semenogelin are responsible for the liquefaction of the semen after ejaculation (63). If the semen is not fully liquefied the high density of seminal plasma impedes the progressive sperm movement. However, in our study we have excluded this type of samples as they were considered as incorrect and not connected directly with motility of spermatozoa. Also, the measurement of the seasonal dependencies was impossible due to our model of isolated asthenozoospermia as seasoning was documented to be also correlated with other sperm pathologies that were excluded from our study (57).

In conclusion, we present here proteomic data supported by two additional mitochondrial tests (JC-1 and MitoSox Red) that plainly indicate the molecular aetiology of AZS. This isolated syndrome, without any additional sperm disturbances, is an advantage of our study. Our results show that low sperm motility is caused mainly by dysfunctional mitochondria and insufficient production of energy (*Fig. 8*). This pathology probably is a result of oxidative stress and ROS activity. The identification of epididymal proteins suggests that this stress can be present in epididymis (and even testis) changing the expression of some proteins during sperm maturation. Additionally, the upregulated expression of some proteins, or their subunits, can be treated as a form of compensation for dysfunctional pathways in AZS. Summing up, these findings contribute to the identification of critical points in cellular metabolism responsible for sperm motility and may therefore have an impact on possible future diagnostic and therapeutic applications in male infertility, while differentiating conditions for conservative treatment versus assisted reproductive techniques.

Conflict of interests: None declared.

REFERENCES

1. Moore FL, Reijo-Pera RA. Male sperm motility dictated by mother's mtDNA. Am J Hum Genet 2000; 67: 543-548.
2. Hwang K, Walters RC, Lipshultz LI. Contemporary concepts in the evaluation and management of male infertility. *Nat Rev Urol* 2011; 8: 86-94.
3. Liu FJ, Liu X, Han JL, et al. Aged men share the sperm protein PATE1 defect with young asthenozoospermia patients. *Hum Reprod* 2015; 30: 861-869.
4. Saraswat M, Joenvaara S, Jain T, et al. Human spermatozoa quantitative proteomic signature classifies normo- and asthenozoospermia. *Mol Cell Proteomics* 2017; 16: 57-72.
5. Asghari A, Marashi SA, Ansari-Pour N. A sperm-specific proteome-scale metabolic network model identifies non-glycolytic genes for energy deficiency in asthenozoospermia. *Syst Biol Reprod Med* 2017; 63: 100-112.
6. Nagata O, Nakamura M, Sakimoto H, et al. Mouse model of chorea-acanthocytosis exhibits male infertility caused by impaired sperm motility as a result of ultrastructural morphological abnormalities in the mitochondrial sheath in the sperm midpiece. *Biochem Biophys Res Commun* 2018; June 21: S0006-291X(18)31408-6. doi: 10.1016/j.bbrc.2018.06.096 [epub ahead of print].
7. Lackner JE, Herwig R, Schmidbauer J, Schatzl G, Kratzik C, Marberger M. Correlation of leukocytospermia with clinical infection and the positive effect of antiinflammatory treatment on semen quality. *Fertil Steril* 2006; 86: 601-605.
8. El-Taieb MA, Herwig R, Nada EA, Greilberger J, Marberger M. Oxidative stress and epididymal sperm transport, motility and morphological defects. *Eur J Obstet Gynecol Reprod Biol* 2009; 144: S199-S203.
9. Herwig R, Knoll C, Planyavsky M, Pourbiabany A, Greilberger J, Bennett KL. Proteomic analysis of seminal plasma from infertile patients with oligoasthenotera-tozoospermiadue to oxidative stress and comparison with fertile volunteers. *Fertil Steril* 2013; 100: 355-366. e2.
10. Sanocka D, Kurpisz M. Reactive oxygen species and sperm cells. *Reprod Biol Endocrinol* 2004; 23: 12. doi: 10.1186/1477-7827-2-12
11. Du Plessis SS, Agarwal A, Halabi J, Tvrda E. Contemporary evidence on the physiological role of reactive oxygen species in human sperm function. *J Assist Reprod Genet* 2015; 32: 509-520.
12. Agarwal A, Mulgund A, Alshahrani S, et al. Reactive oxygen species and sperm DNA damage in infertile men presenting with low level leukocytospermia. *Reprod Biol Endocrinol* 2014; 12: 126. doi: 10.1186/1477-7827-12-126
13. Aitken RJ, Buckingham DW, Brindle J, Gomez E, Baker HW, Irvine DS. Analysis of sperm movement in relation to the oxidative stress created by leukocytes in washed sperm preparations and seminal plasma. *Hum Reprod* 1995; 10: 2061-2071.
14. Negre-Salvayre A, Coatrieux C, Ingueneau C, Salvayre R. Advanced lipid peroxidation end products in oxidative damage to proteins. Potential role in diseases and therapeutic prospects for the inhibitors. *Br J Pharmacol* 2008; 153: 6-20.
15. Ott M, Gogvadze V, Orrenius S, Zhivotovsky B. Mitochondria, oxidative stress and cell death. *Apoptosis* 2007; 12: 913-922.
16. Koppers AJ, Mitchell LA, Wang P, Lin M, Aitken RJ. Phosphoinositide 3-kinase signalling pathway involvement in a truncated apoptotic cascade associated with motility loss and oxidative DNA damage in human spermatozoa. *Biochem J* 2011; 436: 687-698.
17. Amaral A and Ramalho-Santos J. Assessment of mitochondrial potential: implications for the correct monitoring of human sperm function. *Int J Androl* 2010; 33: 180-186.
18. Zhang G, Wang Z, Ling X, et al. Mitochondrial biomarkers reflect semen quality: results from the MARCHS study in Chongqing, China. *PLoS One* 2016; 11: e0168823. doi: 10.1371/journal.pone.0168823
19. Aitken RJ, Whiting S, De Iuliis GN, McClymont S, Mitchell LA, Baker MA. Electrophilic aldehydes generated by sperm metabolism activate mitochondrial reactive oxygen species generation and apoptosis by targeting succinate dehydrogenase. *J Biol Chem* 2012; 287: 33048-33060.
20. Amaral A, Paiva C, Attardo Parrinello C, et al. Identification of proteins involved in human sperm motility using high-throughput differential proteomics. *J Proteome Res* 2014; 13: 5670-5684.
21. WHO Laboratory Manual for the Examination and Processing of Human Semen. World Health Organization, Department of Reproductive Health and Research. Geneva 2010.
22. Fraczek M, Hryhorowicz M, Gaczarzewicz D, et al. Can apoptosis and necrosis coexist in ejaculated human

spermatozoa during in vitro semen bacterial infection? *J Assist Reprod Genet* 2015; 32: 771-779.

23. Martinez-Heredia J, de Mateo S, Vidal-Taboada JM, Ballesca JL, Oliva R. Identification of proteomic differences in asthenozoospermic sperm samples. *Hum Reprod* 2008; 23: 783-791.

24. Pixton KL, Deeks ED, Flesch FM, et al. Sperm proteome mapping of a patient who experienced failed fertilization at IVF reveals altered expression of at least 20 proteins compared with fertile donors: case report. Hum. *Reprod* 2004; 19: 1438-1447.

25. Nowicka-Bauer K, Ozgo M, Lepczynski A, et al. Human sperm proteins identified by 2-dimensional electrophoresis and mass spectrometry and their relevance to a transcriptomic analysis. *Reprod Biol* 2018; 18: 151-160.

26. Pink M, Verma N, Rettenmeier AW, Schmitz-Spanke S. CBB staining protocol with higher sensitivity and mass spectrometric compatibility. *Electrophoresis* 2010; 31: 593-598.

27. Rogowska-Wrzesinska A, Bihan MC, Thaysen-Andersen M, Roepstorff P. 2D gels still have a niche in proteomics. *J Proteomics* 2013; 88: 4-13.

28. Ozgo M, Lepczynski A, Herosimczyk A. Two-dimensional gel-based serum protein profile of growing piglets. *Turk J Biol* 2015; 39: 320-327.

29. Huang da W, Sherman BT, Lempicki RA. Systematic and integrative analysis of large gene lists using DAVID bioinformatics resources. *Nat Protoc* 2009; 4: 44-57.

30. Lemanska-Perek A, Lis-Kuberka J, Lepczynski A, et al. Potential plasma biomarkers of bladder cancer identified by proteomic analysis: a pilot study. *Adv Clin Exp Med* 2019; Jul : doi: 10.17219/acem/79296 [ahead of print].

31. An CN, Jiang H, Wang Q, et al. Down-regulation of DJ-1 protein in the ejaculated spermatozoa from Chinese asthenozoospermia patients. *Fertil Steril* 2011; 96: 19-23.

32. Chan CC, Shui HA, Wu CH, et al. Motility and protein phosphorylation in healthy and asthenozoospermic sperm. *J Proteome Res* 2009; 8: 5382-5386.

33. Majka G, Spiewak K, Kurpiewska K, et al. A high-throughput method for the quantification of iron saturation in lactoferrin preparations. *Anal Bioanal Chem* 2013; 405: 5191-5200.

34. Aitken RJ, Harkiss D, Buckingham D. Relationship between iron catalysed lipid peroxidation potential and human sperm function. *J Reprod Fertil* 1993; 98: 257-265.

35. Kiso WK, Several V, Nagashima J, et al. Biosynthesis of four rat liver mitochondrial acyl-CoA dehydrogenases: in vitro synthesis, import into mitochondria, and processing of their precursors in a cell-free system and in cultured cells. *Arch Biochem Biophys* 1987; 252: 662-674.

36. Ikeda Y, Keese SM, Fenton WA, Tanaka K. Biosynthesis of four rat liver mitochondrial acyl-CoA dehydrogenases: in vitro synthesis, import into mitochondria, and processing of their precursors in a cell-free system and in cultured cells. *Arch Biochem Biophys* 1987; 252: 662-674.

37. Naito E, Ozasa H, Ikeda Y, Tanaka K. Molecular cloning and nucleotide sequence of complementary DNAs encoding human short chain acyl-coenzyme A dehydrogenase and the study of the molecular basis of human short chain acyl-coenzyme A dehydrogenase deficiency. *J Clin Invest* 1989; 83: 1605-1613.

38. Sarto C, Marocchi A, Sanchez JC, et al. Renal cell carcinoma and normal kidney protein expression. *Electrophoresis* 1997; 18: 599-604.

39. Friry-Santini C, Rouquie D, Kennel P, Tinwell H, Benahmed M, Bars R. Correlation between protein accumulation profiles and conventional toxicological findings using a model antiandrogenic compound, flutamide. *Toxicol Sci* 2007; 97: 81-93.

40. Amaral A, Castillo J, Estanyol JM, Ballesca JL, Ramalho-Santos J, Oliva R. Human sperm tail proteome suggests new endogenous metabolic pathways. *Mol Cell Proteomics* 2013; 12: 330-342.

41. Chen Y, Liang P, Huang Y, et al. Glycerol kinase-like proteins cooperate with Pld6 in regulating sperm mitochondrial sheath formation and male fertility. *Cell Discov* 2017; 3: 17030. doi: 10.1038/celldisc.2017.30

42. Shen S, Wang J, Liang J, He D. Comparative proteomic study between human normal motility sperm and idiopathic asthenozoospermia. *World J Urol* 2013; 31: 1395-1401.

43. Roy A, Lin YN, Agno JE, DeMayo FJ, Matzuk MM. Tektin 3 is required for progressive sperm motility in mice. *Mol Reprod Dev* 2009; 76: 453-459.

44. Siva AB, Kameshwari DB, Singh V, et al. Proteomics-based study on asthenozoospermia: differential expression of proteasome alpha complex. *Mol Hum Reprod* 2010; 16: 452-462.

45. Hashemitabar M, Sabbagh S, Orazizadeh M, Ghadiri A, Bahmanzadeh M. A proteomic analysis on human sperm tail: comparison between normozoospermia and asthenozoospermia. *J Assist Reprod Genet* 2015; 32: 853-863.

46. Miki K, Willis WD, Brown PR, Goulding EH, Fulcher KD, Eddy EM. Targeted disruption of the Akap4 gene causes defects in sperm flagellum and motility. *Dev Biol* 2002; 248: 331-342.

47. Luconi M, Cantini G, Baldi E, Forti G. Role of a-kinase anchoring proteins (AKAPs) in reproduction. *Front Biosci* (*Landmark Ed*) 2011; 16: 1315-1330.

48. Pearl CA, Roser JF. Expression of lactoferrin in the boar epididymis: effects of reduced estrogen. *Domest Anim Endocrinol* 2008; 34: 153-159.

49. Wichmann L, Vaalasti A, Vaalasti T, Tuohimaa P. Localization of lactoferrin in the male reproductive tract. *Int J Androl* 1989; 12: 179-186.

50. Wang P, Liu B, Wang Z, Niu X, Su S, Zhang W, Wang X. Characterization of lactoferrin receptor on human spermatozoa. *Reprod Biomed Online* 2011; 22: 155-161.

51. Hamada A, Sharma R, du Plessis SS, et al. Two-dimensional differential in-gel electrophoresis-based proteomics of male gametes in relation to oxidative stress. *Fertil Steril* 2013; 99: 1216-1226.

52. Sharma R, Agarwal A, Mohanty G, et al. Proteomic analysis of seminal fluid from men exhibiting oxidative stress. *Reprod Biol Endocrinol* 2013; 11: 85. doi: 10.1186/1477-7827-11-85.

53. Piomboni P, Gambera L, Serafini F, Campanella G, Morgante G, De Leo V. Sperm quality improvement after natural anti-oxidant treatment of asthenoteratospermic men with leukocytospermia. *Asian J Androl* 2008; 10: 201-206.

54. Saalmann A, Munz S, Ellerbrock K, Ivell R, Kirchhoff C. Novel sperm-binding proteins of epididymal origin contain four fibronectin type II-modules. *Mol Reprod Dev* 2001; 58: 88-100.

55. Sun Y, Zhang WJ, Zhao X, Yuan RP, Jiang H, Pu XP. PARK7 protein translocating into spermatozoa mitochondria in Chinese asthenozoospermia. *Reproduction* 2014; 148: 249-257.

56. Sekito A, Koide-Yoshida S, Niki T, Taira T, Iguchi-Ariga SM, Ariga H. DJ-1 interacts with HIPK1 and affects H_2O_2-induced cell death. Free Radic Res 2006; 40: 155-165.

57. Ozelci R, Yilmaz S, Dilbaz B, et al. Seasonal variation of human sperm cells among 4,422 semen samples: a retrospective study in Turkey. *Syst Biol Reprod Med* 2016; 62: 379-386.

58. Pawlicki P, Milon A, Zarzycka M, et al. Does signaling of estrogen-related receptors affect structure and function of bank vole Leydig cells? *J Physiol Pharmacol* 2017; 68: 459-476.

59. Deng SL, Sun TC, Yu K, et al. Melatonin reduces oxidative damage and upregulates heat shock protein 90 expression in cryopreserved human semen. *Free Radic Biol Med* 2017; 113: 347-354.

60. Kratz EM, Piwowar A. Melatonin, advanced oxidation protein products and total antioxidant capacity as seminal parameters of prooxidant-antioxidant balance and their connection with expression of metalloproteinases in context of male fertility. *J Physiol Pharmacol* 2017; 68: 659-668.

61. Lu XL, Liu JJ, Li JT, Yang QA, Zhang JM. Melatonin therapy adds extra benefit to varicecelectomy in terms of sperm parameters, hormonal profile and total antioxidant capacity: a placebo-controlled, double-blind trial. *Andrologia* 2018; 8: e13033. doi: 10.1111/and.13033

62. Al-Maghrebi M, Renno WM. Genistein alleviates testicular ischemia and reperfusion injury-induced spermatogenic damage and oxidative stress by suppressing abnormal testicular matrix metalloproteinase system via the Notch 2/Jagged 1/Hes-1 and caspase-8 pathways. *J Physiol Pharmacol* 2016; 67: 129-137.

63. Shimokawa Ki K, Katayama M, Matsuda Y, et al. Matrix metalloproteinase (MMP)-2 and MMP-9 activities in human seminal plasma. *Mol Hum Reprod* 2002; 8: 32-36.

Author's address: Prof. Maciej Kurpisz, Department of Reproductive Biology and Stem Cells, Institute of Human Genetics, Polish Academy of Sciences, 32 Strzeszynska Street, 60-479 Poznan, Poland.
E-mail: kurpimac@man.poznan.pl